Arab J. Nucl. Sci. Appl., Vol. 55, 2, 113-124 (2022)

ISSN 1110-0451

Arab Journal of Nuclear Sciences and Applications

Web site: ajnsa.journals.ekb.eg

(E S N S A)

Radioactivity and Radionuclide Distribution in Jabel Bawr Oil Site of Kirkuk-Iraq

Ali H. Taqi* and Berivan F. Namq

Department of Physics, College of Science, Kirkuk University, Kirkuk, Iraq

ARTICLE INFO

Article history:

Received: 30th Aug. 2021

Accepted: 17th Nov. 2021

Keywords:

Natural and artificial radioactivity,

Activity concentration,

Radiological hazard.

ABSTRACT

Everything around us is continuously exposed to the radiation of the Naturally Occurring (NORM) such as cosmic rays and terrestrial radioactive elements. However but human and technological activities may contribute to increasing the effect causing what is called the Technologically Enhanced Naturally Occurring Radioactive Materials (TENORM) In the present Radioactive Materials investigation, the radioactivity in soil samples from Jabal Bawr oil site of Kirkuk-Iraq have been studied using a high purity germanium (HPGe) detector. The specific activity of ^{226}Ra, ^{232}Th, ^{40}k and ^{137}Cs varied between 24.4-68 Bq kg^{-1}, 11.6-27.2 Bq kg^{-1}, 207.2-591 Bq kg^{-1} and BDL-2.40 Bq kg^{-1} respectively. The hazard indices (the radium equivalent activity, the absorbed gamma dose rate, the annual effective dose rate, the external and internal hazards, the Gamma radiation representative level index, and excess lifetime cancer risk have been calculated. The results obtained of some sites were found to be higher than the allowable worldwide values. Statistical analysis has been implemented to explain the obtained results.

1. INTRODUCTION

Naturally Occurring Radioactive Materials (NORM) have been found in the soil, rocks, water, and building materials. Radionuclides such as ^{238}U and ^{232}Th or their progeny, as well as ^{40}K, can be traced back to the prehistoric era [1]. It is unavoidable for humans to be exposed to ionising radiation. External radiation exposure is caused by both natural and man-made radioactivity. Ionizing radiation interacts with the human body, causing a variety of biological effects that may manifest as clinical symptoms [2].

Measurements of soil radioactivity levels are important for understanding changes in the natural radiation background as a function of geographical location and time, and also in forming the basis for the assessment of the degree of the radioactive contamination or pollution in the environment in the future [3, 4].

The current study aims at evaluate the specific activity of ^{226}Ra, ^{232}Th, ^{40}k and ^{137}Cs in soil samples collected from Jable Bawr oil site of Kirkuk-Iraq . The hazard indices: the radium equivalent activity (Ra_{eq}), the absorbed dose (D), Gamma radiation representative level index (I_γ), the external hazard and internal hazard index (H_{ex}, H_{in}), the annual effective dose rate (AEDE), and excess lifetime cancer risk (ELCR) have also been calculated. Statistical analysis has been also implemented to explain the obtained results.

2. EXPERIMENTAL TECHNIQUES

In the present study, soil samples were selected from Jabel Bawr oil field of Kirkuk-Iraq which is distributed around oil wells. The locations of the investigated samples are shown in Fig. (1). The samples were taken at the chosen point from a depth of 45 cm labelled, then mixed, sieved through 0.25-mm mesh, dried at 100 ^{0}C for 24 hours, placed in polyethylene containers, and finally were stored at least 4 weeks to ensure the radioactive equilibrium between radon and its decay products [5].

The acquisition time of each sample was 3600 sec in the gamma energy transition rang ~ 1000 keV-2614 keV which is performed using a high-purity germanium (HPGe) detector and spectroscopy system. The specific activities of the 232Th was determined using gamma-ray transition lines of 228Ac and 212Pb, while the specific activity of 226Ra and 214Pb were used to determine the activity of 238U, gamma transition peaks of 40K and 137Cs were determined at 1461 and 662 keV, respectively.

Corresponding author: alitaqibayati@yahoo.com

DOI: 10.21608/ajnsa.2021.93425.1508

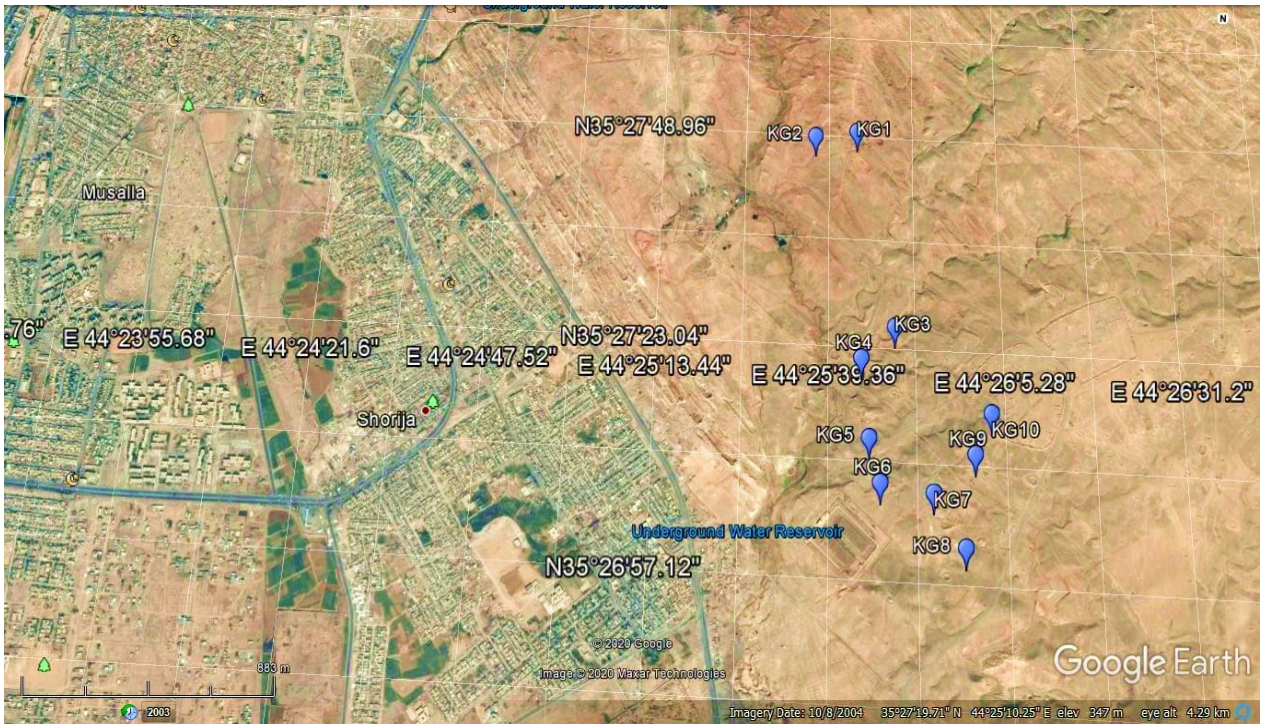

Fig. (1): Locations of the investigated samples

3. Estimation of activity and hazard indices

The specific activity of the investigated samples is obtained using the following equation [6]:

$$A\ (Bq\ kg^{-1}) = \frac{C_{net}}{\varepsilon(E_\gamma)\times I_\gamma \times m(kg)} \quad \textbf{(1)}$$

Where C_{net} is the net peak count rate (Count Sec^{-1}), I_γ is the probability of the emission of the gamma line corresponding to the peak energy, ε is the absolute efficiency at photo peak energy.

The Radium activity equivalent (Ra_{eq}) is widely used to determine the hazards index in terms of the activities of the ^{226}Ra, ^{232}Th and ^{40}K as explained by the following[7]:

$$Ra_{eq} = A_{Ra} + 1.43A_{Th} + 0.077A_k \quad \textbf{(2)}$$

The absorbed dose rate (D) in nGy h^{-1}can be determined using the following relation [8-10]:

$$D = 0.462A_{Ra} + 0.604A_{Th} + 0.0417A_K \quad \textbf{(3)}$$

The external and internal hazard indices (H_{ex} and H_{in}) were measured by the following equation [11]:

$$H_{ex} = \frac{A_{Ra}}{370} + \frac{A_{Th}}{259} + \frac{A_K}{4810} \leq 1 \quad \textbf{(4)}$$

$$H_{in} = \frac{A_{Ra}}{185} + \frac{A_{Th}}{259} + \frac{A_K}{4810} \leq 1 \quad \textbf{(5)}$$

The representative level index (Iγ) is used for measuring gamma radiation in soil correlated with the natural radionuclide. This is defined by the following[12]:

$$I_\gamma = \frac{A_{Ra}}{150} + \frac{A_{Th}}{100} + \frac{A_K}{1500} \leq 1 \quad \textbf{(6)}$$

In order to calculate the annual effective dose equivalent at air, the outdoor occupancy factor of about 0.2 and the conversion coefficient of 0.7 Sv Gy^{-1} which is used to convert the absorbed dose rate (D) in air (in nGy h^{-1}) to the effective dose equivalent in (Sv y^{-1}) obtained by adults (female and male) must be taken into consideration. The average annual mean effective dose worldwide is 460 μSv y^{-1} [10]. AEDE in mSv y^{-1} is computed by the following equations:

$$AEDE_{out} = D \times 8760 \times 0.2 \times 0.7 \times 10^{-6} \quad \textbf{(7)}$$

$$AEDE_{in} = D \times 8760 \times 0.8 \times 0.7 \times 10^{-6} \quad \textbf{(8)}$$

The excess lifetime cancer risk (ELCR) is caused by ionising radiation exposure over a lifetime [13, 14]:

$$ELCR = AEDE \times DL \times RF \quad \textbf{(9)}$$

Where DL is the average life span (70 years) and RF (Sv^{-1}) fatal risk factor per Sievert, which is 0.057 as per the International Commission on Radiological Protection[15].

4. RESULTS AND DISCUSSION

4.1 Specific activity hazard indices

The specific activity of ^{226}Ra (series of ^{238}U), ^{228}Ac (series of ^{232}Th), non-series (^{40}K) and ^{137}Cs of the investigated 10 soil samples are depicted in Figs (2 to 4 respectively). Table (1). shows the specific activity and average values of ^{226}Ra, ^{232}Th, ^{40}K and ^{137}Cs.

The range of the specific activity of ^{226}Ra was 24.4-68 Bq kg^{-1} with an average of 46.30 Bq kg^{-1}. The minimum value is obtained in KG1 and the maximum value is obtained in KG4. The higher values were for the sites closest to the oil wells. In general, the geochemical composition and origin of the soil types are also attributable to the radioactivity. The range of the measured specific activity of ^{232}Th was 11.6-27.2 Bq kg^{-1} with an average of 22.10 Bq kg^{-1}. The minimum value is obtained in KG9 and the maximum value is obtained in KG5 and KG10. The differences were significant in all samples depending on the distance from the oil wells. The specific activity of ^{40}K was 207.2-591 Bq kg^{-1} with an average 387.07 Bq kg^{-1}. The minimum value is obtained in KG7 and the maximum value is obtained in KG10. The difference are also attributable to the soil type differences in the region under investigation value besides the industrial oil waste. In addition, contour maps of the specific activity are presented in Figs. (5, 6 and 7).

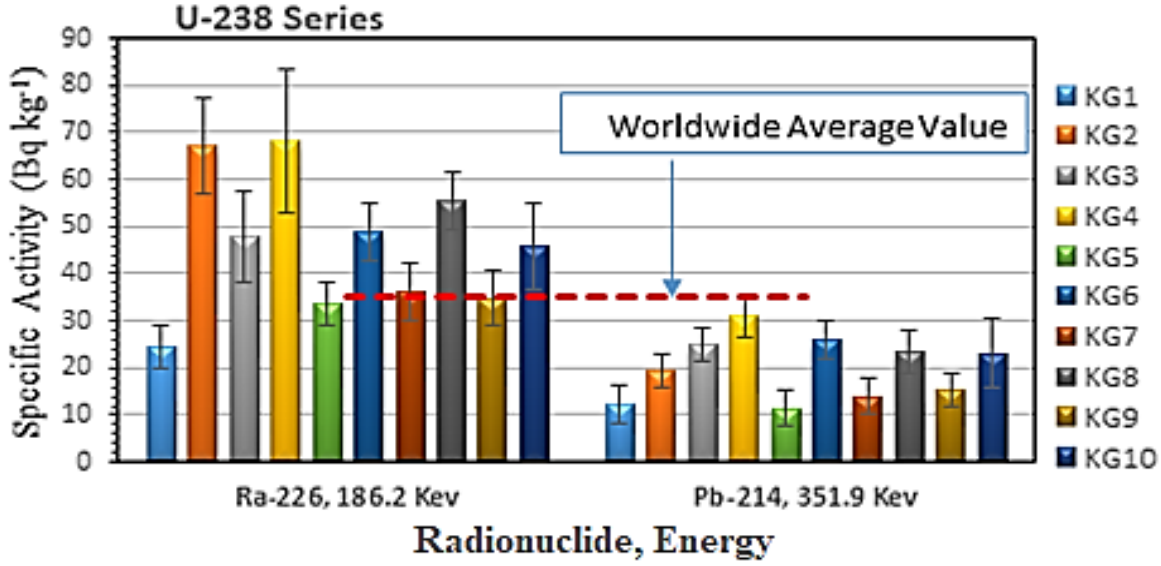

Fig. (2): specific activity of ^{238}Useries of the investigated soil samples in comparison with the worldwide average value

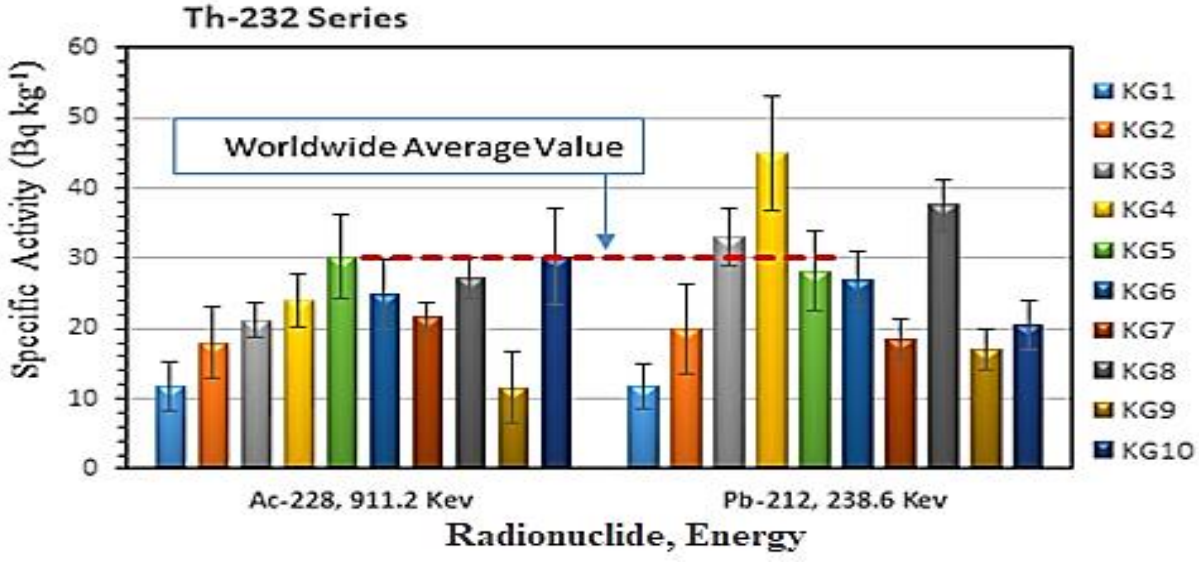

Fig. (3): specific activity of ^{232}Th series of the investigated soil samples in comparison with the worldwide average value

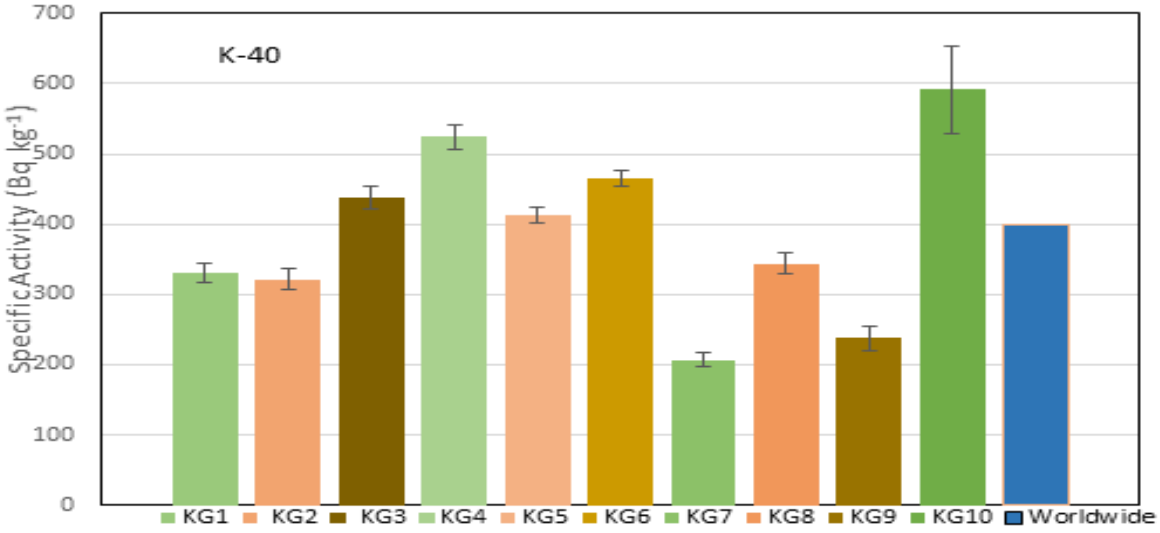

Fig. (4): specific activity of ^{40}K series of the investigated soil samples in comparison with the worldwide average value

Table (1): Specific activity (Bq kg^{-1}) of the selected samples of Jabel Bawr field. BDL: Below Detection Limit.

Sample ID	^{226}Ra	^{232}Th	^{40}K	^{137}Cs
KG1	24.4±4.4	11.8±3.5	330.0±14.3	BDL
KG2	67.0±10.2	18.0±5	321.2±14.9	2.40±0.3
KG3	48.0±9.7	21.2±2.5	437.6±16	BDL
KG4	68.0±15.3	24.0±3.9	524.2±17	BDL
KG5	33.8±4.6	30.2±6	413.0±11.6	BDL
KG6	48.9±6	24.8±5	464.8±11	BDL
KG7	36.2±6.3	21.7±2.1	207.2±10.6	BDL
KG8	55.6±6.2	27.2±2.8	343.8±15.5	BDL
KG9	34.8±5.8	11.6±5	237.9±17	BDL
KG10	45.8±9.1	30.2±6.9	591.0±62	BDL
Range	24.4-68	11.6-27.2	207.2-591	BDL-2.40
Average	46.30	22.10	387.07	2.40

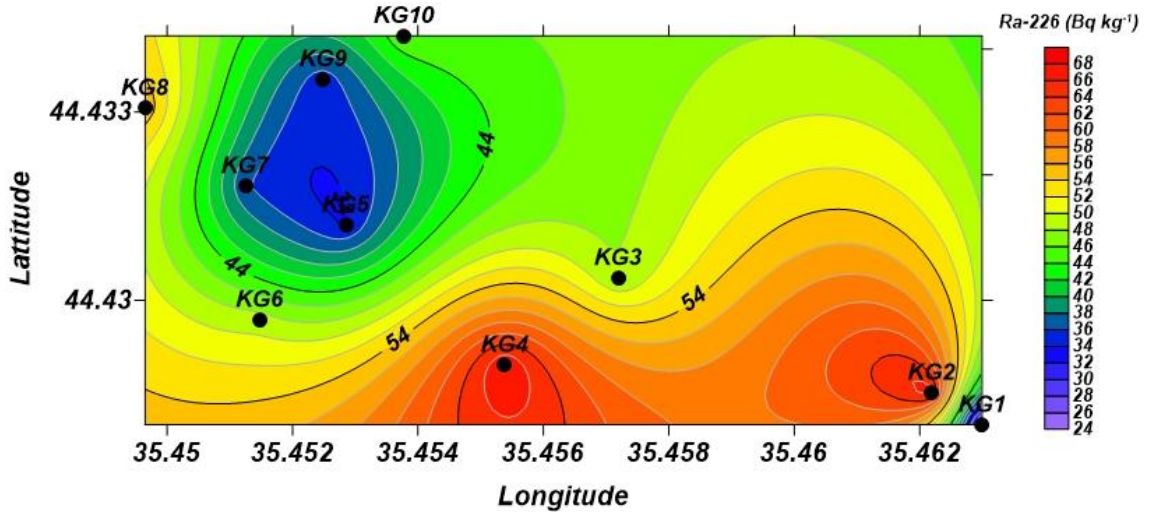

Fig. (5): a contour map of the sample locations and how the specific activity of ^{226}Ra are distributed

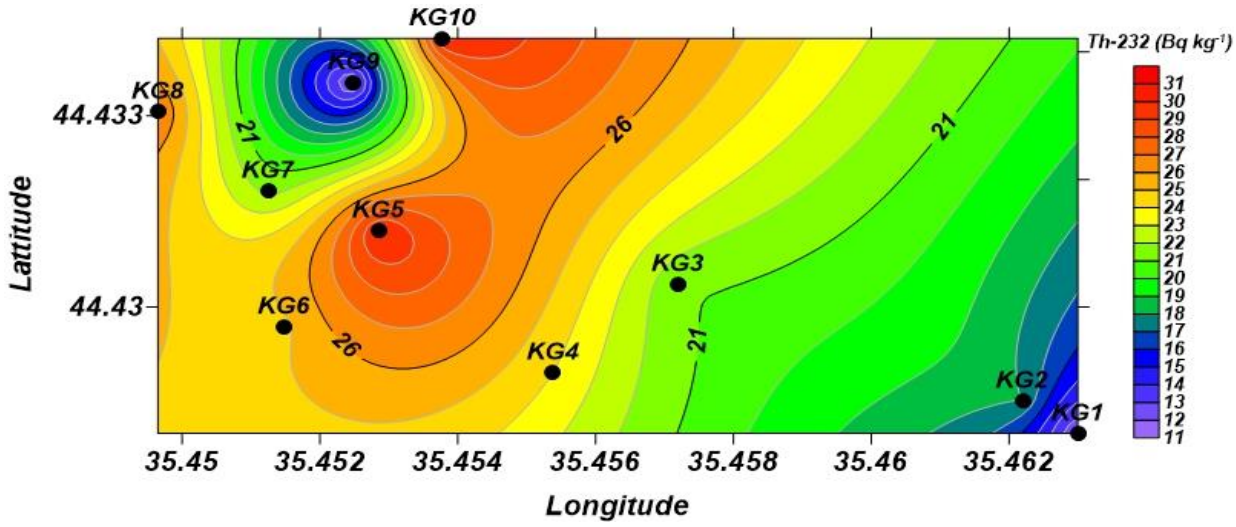

Fig. (6): a contour map of the sample locations and how specific activity of the ^{232}Th are distributed

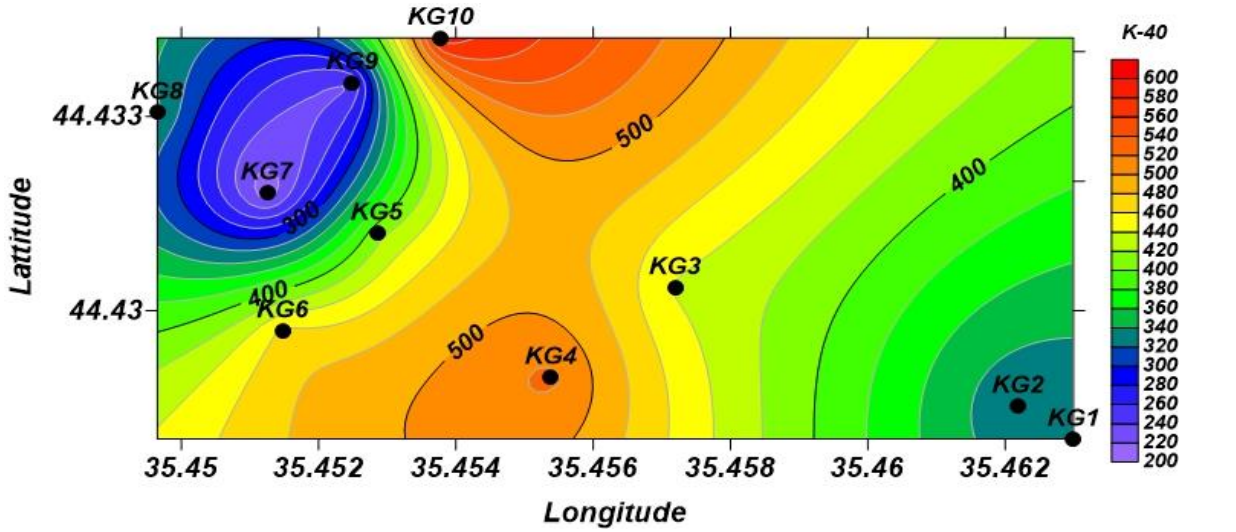

Fig. (7): a contour map of the sample locations and how the specific activity of ^{40}K are distributed

The measured specific activities of the investigated soil samples are compared with those of the previous studies as presented in Table (2). The specific activities of ^{226}Ra and ^{232}Th reported in previous studies [16], [17] and [18] were higher than the values of the present study. The maximum value of ^{40}K activity in the present study is much lower than those reported in earlier publications [10], [17], [16], [18], [19], [20], [21] and [22]. The high recorded values of the radionuclides in some soil samples are attributed to the geochemical composition and the samples were collected from the areas around the oil wells.

The obtained radiological hazard indices are illustrated in Table (3). The value of Ra_{eq} varied from 66.68-134.49 Bq kg^{-1} with an average value of 107.61 Bq kg^{-1}. The D values varies from 32.16 to 67.77 nGy h^{-1} with an average value of 50.84 nGy h^{-1}.

The range of the calculated H_{ex} was 0.18-0.39 with an average value of 0.29, where the average value is less than 1. The H_{in} ranged between 0.25 and 0.57 with an average value less than 1.

The range of the calculated I_γ values was 0.50 to1.04 with an average 0.79. The I_γ values for the studied soil samples have higher values than the world average for the samples KG4 and KG10.

The calculated AEDE values in the present study are listed in Table (3). The results of outdoor effective dose were 0.04-0.08 mSv y^{-1} with an average value 0.06 mSv y^{-1}. The results of indoor effective dose were 0.16-0.33 mSv y^{-1} with an average value of 0.25 mSv y^{-1} where the worldwide average values of 0.08 and 0.42 mSv y^{-1} [10]. It appears from all the samples that they reached outdoor and indoor (AEDE) less than the Worldwide value

The range of the ELCR values was 0.16 ×10^{-3} -0.33 ×10^{-3}, where a mean value 0.25×10^{-3} is higher than the world average value 0.29×10^{-3} [10].

Table (2): Range of the specific activity (Bq kg^{-1}) of the selected samples in comparison with previous studies

Country	^{226}Ra	^{232}Th	^{40}K	*References*
Iraq	21.01-63.33	16.65-42.95	245.05-798.52	[19]
Iraq	18.40-312.80	9.40-140.80	66.40-800.80	[16]
Iraq	18.56-62.53	15.31-25.88	403.12-684.32	[20]
Egypt	4.00-48.00	8.00-50.00	16.00-487.00	[22]
Nigeria	54.50-94.20	33.30-71.20	462.10-712.40	[21]
Pakistan	21.37-110.51	11.65-172.06	173.96-825.43	[17]
Iran	8.00-55.00	5.00-42.00	250.00-980.00	[10]
USA	8.00-160.00	4.00-130.00	100.00-700.00	[18]
Worldwide Average	35.00	30.00	400.00	[10]
This Study	24.4-68	11.6-27.2	207.2-591	

Table (3): Radiological hazard indices of the investigated soil samples

Sample ID	Ra_{eq} (Bq Kg^{-1})	D (nGy h^{-1})	H_{ex}	H_{in}	I_γ	$AEDE_{out}$ (mSv y^{-1})	$AEDE_{in}$ (mSv y^{-1})	ELCR ($\times 10^{-3}$)
KG1	66.68	32.16	0.18	0.25	0.50	0.04	0.16	0.16
KG2	117.47	55.22	0.32	0.50	0.84	0.07	0.27	0.27
KG3	112.01	53.23	0.30	0.43	0.82	0.07	0.26	0.26
KG4	142.68	67.77	0.39	0.57	1.04	0.08	0.33	0.33
KG5	108.79	51.08	0.29	0.39	0.80	0.06	0.25	0.25
KG6	120.15	56.95	0.32	0.46	0.88	0.07	0.28	0.28
KG7	83.19	38.47	0.22	0.32	0.60	0.05	0.19	0.19
KG8	120.97	56.45	0.33	0.48	0.87	0.07	0.28	0.28
KG9	69.71	33.00	0.19	0.28	0.51	0.04	0.16	0.16
KG10	134.49	64.05	0.36	0.49	1.00	0.08	0.31	0.31
Range	66.68-134.49	32.16-67.77	0.18-0.39	0.25-0.57	0.50-1.04	0.04-0.08	0.16-0.33	0.16-0.33
Average	107.61	50.84	0.29	0.42	0.79	0.06	0.25	0.25
World Average	370	57	≤1	≤1	≤1	0.08	0.29	0.29

4.2 Multivariate statistical analysis

In the present work, the statistical analysis has been carried out using the statistics software package SPSS version 23.0 for windows. A box plot describes how the specific activities are spread out, while the Cluster analysis and Pearson correlation aim at clarifying the relationship between the statistical variables [23]. In addition, the Principal Component Analysis (PCA) is used to summarize patterns among variables in multivariate datasets, where it is used to identify patterns in variables and to express data in such a way as to highlight their similarities and differences.

4.2.1 Basic statistics

Basic statistical variables: mean, median, kurtosis, deviation, and standard deviation of the parameters were measured and listed in Table (4). kurtosis is a measure of the peak of a real-valued random Variable's probability distribution, compared with the usual distribution, it characterizes the relative peak or flatness of a distribution. Positive kurtosis indicates a relatively peaked distribution. Negative kurtosis indicates a relatively flat distribution. In the present study, the kurtosis of ^{226}Ra (-0.804), ^{232}Th (-0.743) and ^{40}K (-0.680) were found all the radionuclides to have the negative kurtosis which indicate relatively flat distribution, while positive kurtosis of indicated relatively peaked distribution [24]. The skewness of ^{232}Th was negative (-0.494), while ^{226}Ra and ^{40}K were positive (0.241 and 0.152, respectively).

4.2.2 Box plot

The Box plot of how activity concentration spread out for ^{226}Ra, ^{232}Th and ^{40}K in Bq kg^{-1} is given in Fig. (8). The median is near the center of the ^{226}Ra and ^{232}Th box, while the median of the ^{40}K is closer to the bottom of the box, and the distribution is skewed [25].

4.2.3 Frequency distribution and Q-Q plot

The frequency distribution and Quantile-quantile (Q-Q) plots of the specific activity for ^{226}Ra, ^{232}Th and ^{40}K were analyzed and histograms are given in Fig. (9, 10 and 11, respectively). The distribution of ^{40}K, ^{226}Ra and ^{232}Th radionuclides appears to be normal (bell shape distribution). The multimodality characteristics shows the complexity of radionuclides in soil samples. The Q-Q plot is shown in the Figs. (9, 10 and 11), all points lie approximately along the 45-degree reference line; the distributions may be assumed to be normal.

Table (4): Statistical variables of the studied samples

Variables	^{226}Ra	^{232}Th	^{40}K
Mean	46.250	22.070	387.070
Median	46.900	22.850	378.400
Std. Deviation	14.3986	6.6853	121.8983
Variance	207.318	44.693	14859.191
Skewness	0.241	-0.494	0.152
Kurtosis	-0.804	-0.743	-0.680
Minimum	24.4	11.6	207.2
Maximum	68	30.2	591
Range	43.6	18.6	383.8

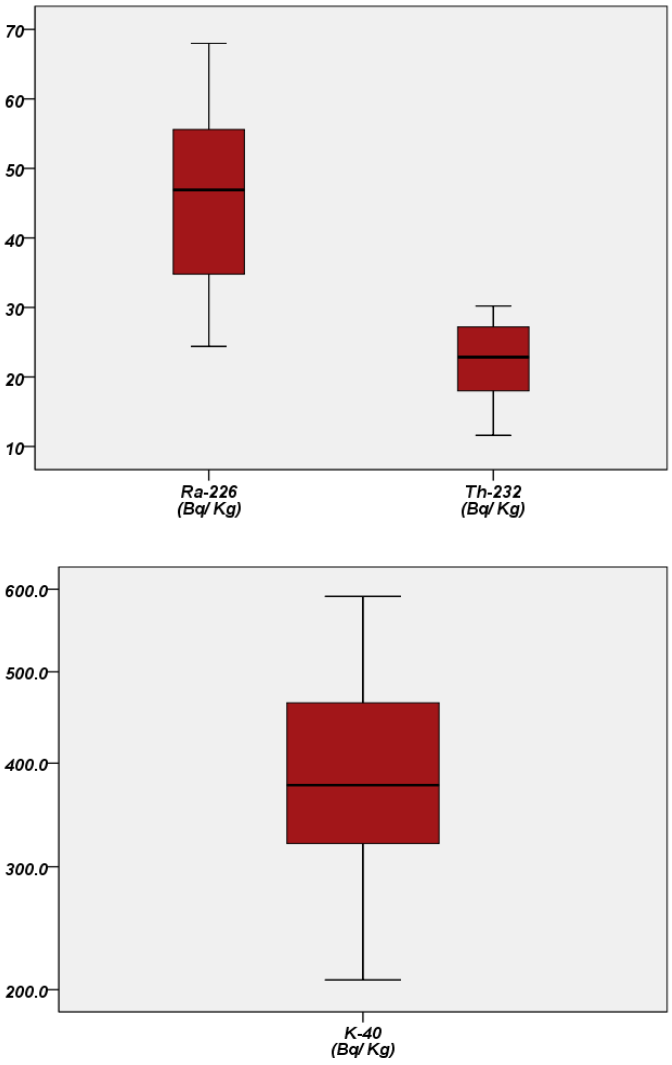

Fig. (8): Box plot of ^{226}Ra, ^{232}Th and ^{40}K of the investigated soil samples

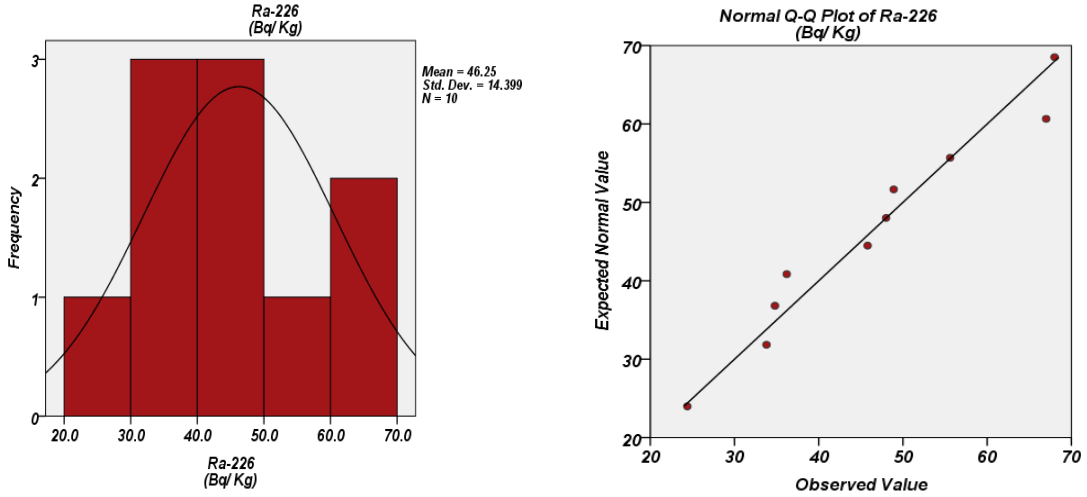

Fig. (9): Frequency distribution and Quantile-quantile (Q-Q) plots of the specific activity for ^{226}Ra of the investigated soil samples

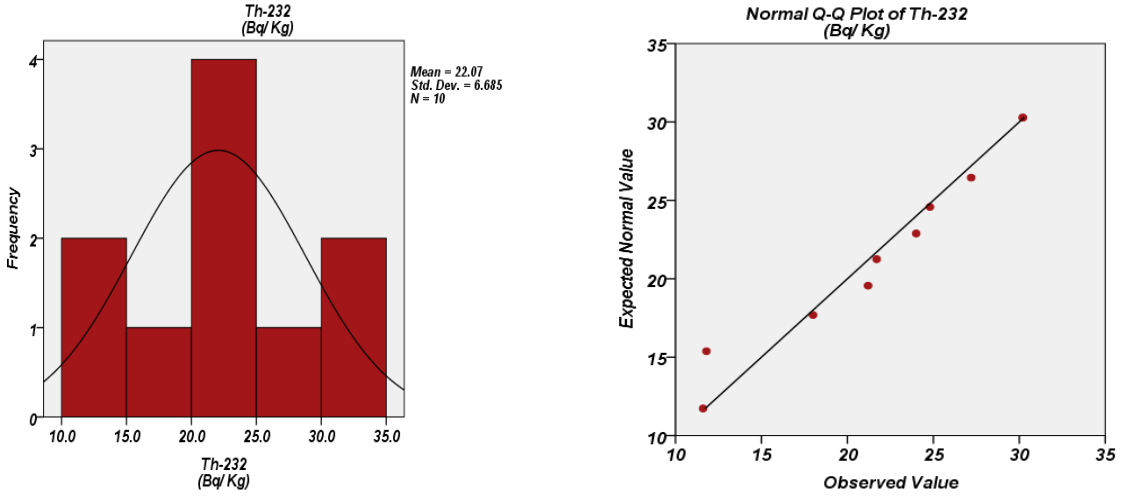

Fig. (10): Same as Fig. 9 for ^{232}Th

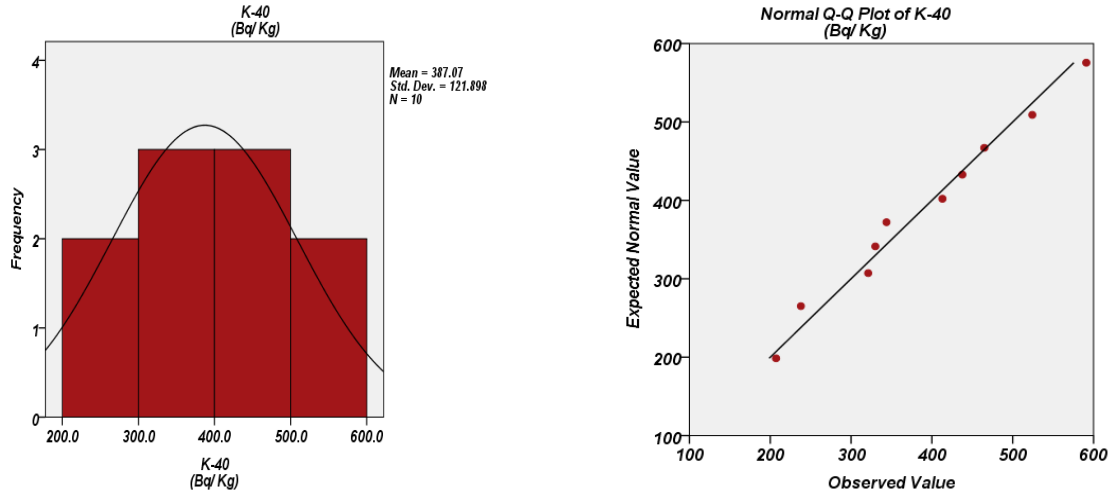

Fig. (11): Same as Fig. 9 for ^{40}K

4.2.4 Pearson's correlation coefficient analysis

Pearson's correlation coefficient analysis was carried out to determine the mutual relationship and strength between pairs of variables, as shown in Table (5). It was found that ^{232}Th has a weak correlation with ^{226}Ra (r=+0.294) and the ^{40}K has a moderate correlation with ^{232}Th (r=0.622).

4.2.5 Principal component analyses

The Principle component analysis (PCA) was applied to identify variables by applying varimax rotation with the Kaiser Normalization Method [26]. The component 1 and component 2 rotation space is illustrated in Table(6) and Fig. (12), where 49.226% of the total variance was the first factor, and mainly characterized by high positive loading of ^{226}Ra and ^{40}K concentrations. The second factor is accounted for 47.024% of the total variance and mainly consisted of positive loading of ^{232}Th. It could be concluded that ^{226}Ra and ^{40}K dominantly increase the radioactivity in the investigate soil samples

4.2.6 Cluster analysis

Cluster Analysis (CA) is used to identify and classify groups with similar features in new observation [25, 27]. The CA was carried out using axes to identify similar characteristics between natural radioisotopes and radiological parameters in soils. In the CA, the average linkage method along with the correlation coefficient distance was applied and the derived dendrogram is shown in Fig.(13) and Table (7) shows the cluster membership, where the variables are grouped in three stages as shown in the Table (7). All the 10 parameters are grouped in four statistically significant clusters. Clusters-I constant of ^{226}Ra; cluster II was ^{232}Th; cluster III was ^{40}K and cluster IV consisted of other radiological parameters distribution, which appeared in the same cluster in the first stage. Three clusters were included in the second stage, where the variables of the fourth cluster were merged with the first cluster. In the third stage, the variables of the third cluster were merged with those of the first cluster, thus there are only two clusters, the first and the second. In the last phase, all the cluster were merged with the second cluster.

Table (5): correlation matrix of the studied soil samples

Variables	^{226}Ra	^{232}Th	^{40}K	Ra_{eq}	D	H_{ex}	H_{in}	I_γ	$AEDE_{out}$	ELCR
^{226}Ra	1	0.294	0.371	0.794	0.787	0.794	0.911	0.762	0.787	0.787
^{232}Th	0.294	1	0.622	0.753	0.741	0.753	0.619	0.761	0.741	0.741
^{40}K	0.371	0.622	1	0.793	0.814	0.793	0.675	0.828	0.814	0.814
Ra_{eq}	0.794	0.753	0.793	1	0.999	1	0.974	0.998	0.999	0.999
D	0.787	0.741	0.814	0.999	1	0.999	0.971	0.999	1	1
H_{ex}	0.794	0.753	0.793	1	0.999	1	0.974	0.998	0.999	0.999
H_{in}	0.911	0.619	0.675	0.974	0.971	0.974	1	0.961	0.971	0.971
I_γ	0.762	0.761	0.828	0.998	0.999	0.998	0.961	1	0.999	0.999
$AEDE_{out}$	0.787	0.741	0.814	0.999	1	0.999	0.971	0.999	1	1
ELCR	0.787	0.741	0.814	0.999	1	0.999	0.971	0.999	1	1

Table (6): Rotated factors loading of the variables.

Variables	Component	
	1	2
^{226}Ra	0.993	0.107
^{40}K	0.305	0.843
^{232}Th	0.178	0.892
Ra_{eq}	0.724	0.690
AEDE	0.718	0.696
H_{ex}	0.724	0.690
H_{in}	0.861	0.507
I_{γ}	0.690	0.724
D	0.718	0.696
ELCR	0.718	0.696

Table (7): Cluster Membership

Variables	Cluster Membership		
	4 Clusters	3 Clusters	2 Clusters
^{226}Ra	1	1	1
^{40}K	3	3	1
^{232}Th	2	2	2
Ra_{eq}	4	1	1
$AEDE_{out}$	4	1	1
H_{ex}	4	1	1
H_{in}	4	1	1
I_{γ}	4	1	1
D	4	1	1
ELCR	4	1	1

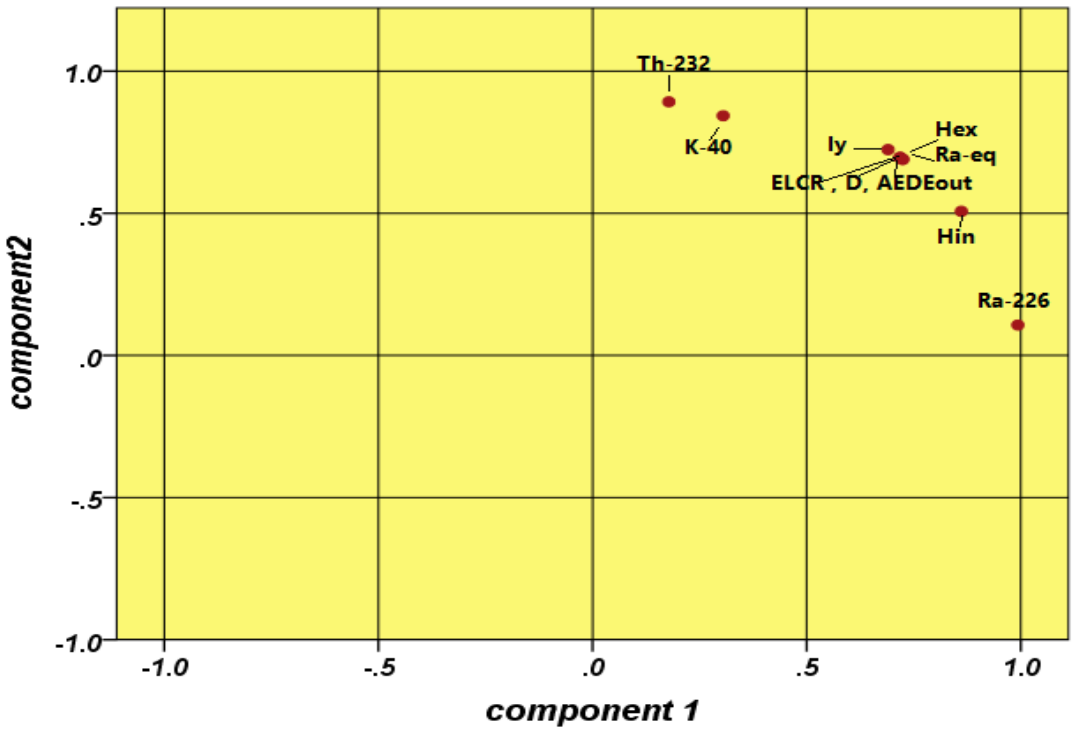

Fig. (12): Graphical representation of Components 1 and 2

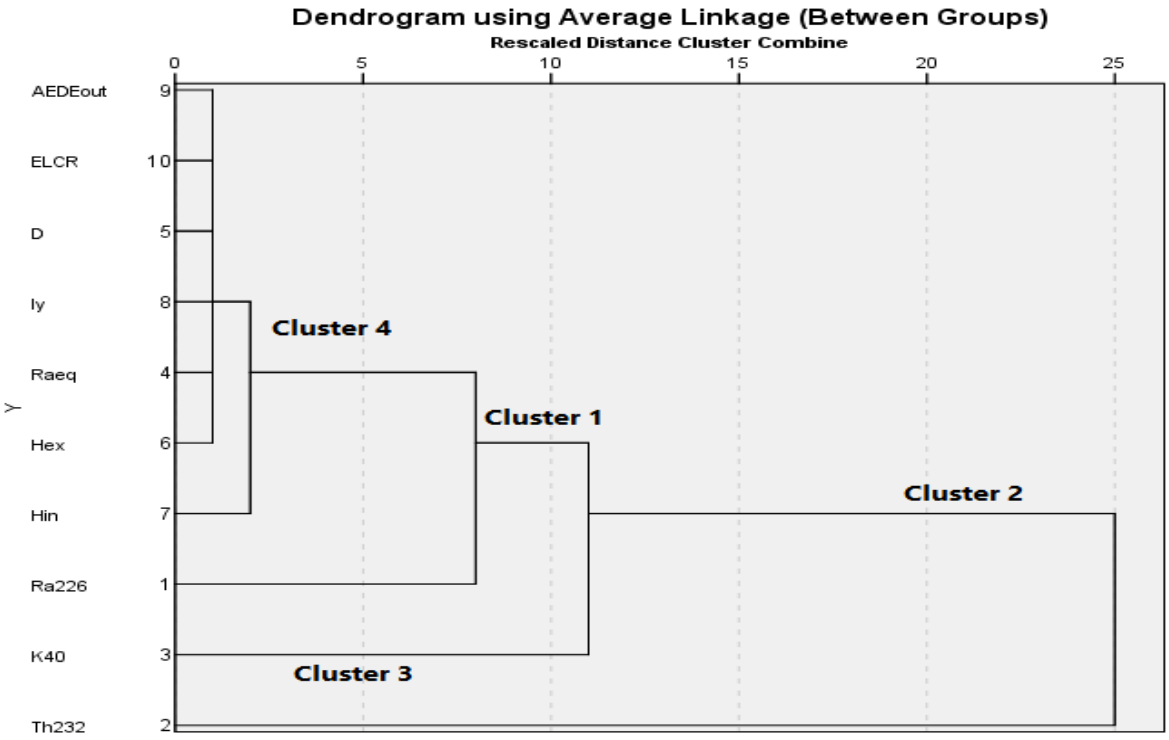

Fig. (13): clustering of radiological parameters

5. CONCLUSION

The measured specific activity of ^{40}K is higher than that of both ^{226}Ra and ^{223}Th. This indicates that ^{40}K is a more abundant than the other radioactive elements of the studied soils. In general, the specific activity of many samples was higher than the recommended worldwide values, because the samples were collected from around oil wells. The average values of the radium equivalent activity (Ra_{eq}) are lower than the international recommended maximum value (370 Bq kg^{-1}). The absorbed gamma dose rate is higher than the world average value. The results of the outdoor effective dose were 0.04 to 0.08 mSv y^{-1} with an average value 0.06 mSv y^{-1}. The calculated outdoor effective dose has lower values than the world average value 0.08 mSv y^{-1} for some locations. The results of indoor effective dose were 0.16 to 0.33 mSv y^{-1} with an average value 0.25 mSv y^{-1}. The calculated indoor effective dose was less than the world average value 0.42 mSv y^{-1}. The excess lifetime cancer risk of the soil samples varies from 0.16 $\times 10^{-3}$ to 0.33×10^{-3} with a mean value 0.25×10^{-3} to be higher than the world average ELCR value of 0.29×10^{-3}.

REFERENCES

[1] M.S. Yasir, A. Ab Majid, R. Yahaya (2007). Study of natural radionuclides and its radiation hazard index in Malaysian building materials. Radio anal. Nucl. Chem, 273, 539-541.

[2] ICRP (1990) Recommendations if the International commission of Radiological Protection. Annals of the ICRP 21, 1-3.

[3] S. V. Bara, Vishal Arora, S. Chinnaesakki, S. J. Sartandel, B.S. Bajwa, R. M. Tripathi, V. D. Puranik (2012). Radiological assessment of natural and fallout radioactivity in the soil of Chamba and Dharamshala areas of Himachal Pradesh, India. Radioanal. Nucl. Chem, 291, 769-776.

[4] A. Kurnaz, B. KüÇükÖmeroğlu, R. Keser, N.T. Okumusoglu, F. Korkmaz, G. Karahan, U. Çevik (2007). Determination of Radioactivity Levels and Hazards of soil and sediment samples in Firtina Valley (Rize, Turkey). Appl. Radiat. Isotopes, 65, 1281-1289.

[5] Quindos L.S., Fernandez P.L., Soto J., Rodenas C. and Comez (1994), J. Natural Radioactivity in Spanish Soils, Health Physics 66, 196-200.

[6] Akôzcan S, Külahci F, Mercan Y (2018). A suggestion to radiological hazards characterization of ^{226}Ra, ^{223}Th , ^{40}K and ^{137}Cs . spatial distribution modelling. J Hazard Mater 353, 476-489.

[7] Beretka J, Mathew P. J (1995). Natural radioactivity of Australian building materials, industrial wastes and byproducts. Health Phys 48, 87-95.

[8] Ali H. Taqi, A.M. Shaker, A. A. Battawy (2018). Natural radioactivity assessment in soil samples from Kirkuk city of Iraq using HPGe detector. International Journal of Radiation Research, 16(4), 455-463.

[9] Ali H. Taqi, A. M. Shaker, A. A. Battawy (2018). Natural radioactivity in Building Materials from Kirkuk city of Iraq. Journal of Radiation and Nuclear Application, 3(3), 199-203.

[10] UNSCEAR (2000) Sources and effects of ionizing radiation. In United Nations Scientific Committee on the effect of atomic radiation, U.N., NY (ed). New York.

[11] Zalina Laili, Mohd Zaidi Ibrahim, Nur Azna Mahmud and Muhamat Omar (2012). Natural Radioactivity Content and Radionuclides Lechability of Bricks Containing Industrial Waste, Agensi Nuklear Malaysia, 26-28.

[12] Nur Nazihah Hassan, Kok Siong Khoo (2014). Measurement of Natural Radioactivity and Assessment of Radiation Hazard Indices in Soil Samples at Pengerang, Kota Tinggi, Johor, Aip Conference Proceedings 1584,190; https:// doi.org/10.1063/1.4866130.

[13] Taskin H, Karavus M, Ay P, Topuzoglu A, Hindiroglu S, Karahan G (2009). Radionuclide concentrations in soil and lifetime cancer risk due to gamma radioactivity in Kirklareli, Turkey. J Environ Radioact 100(1): 49-53.

[14] Kolo M. T., Amin Y. M. , Khandaker M. U., Abdullah W. H. B. (2017). Radionuclide concentration and excess lifetime cancer risk due to gamma radioactivity in tailing enriched soil around Maigannga coal mine, Northeast Nigeria. International Journal of Radiation Research 15(1), 71.

[15] ICRP (2007). The 2007 recommendations of the International Commission on Radiological Protection. ICRP publication 103, Ann. ICRP 37, 1-332.

[16] Kamal K. Ali, Shafik Sh. Shafik, Husain A. Husain (2017). Radiological Assessment of NORM Resulting from Oil and Gas Production Processing in South Rumaila Oil Field, Southern Iraq. Iraq Journal of Science 58(2c), 1037-1050.

[17] Qureshi AA, Tariq S, Din KU, Manzoor S, Calligaris C, Wahhed A (2014). Evaluation of excessive lifetime cancer risk due to natural radioactivity in the rivers sediments of Northern Pakistan. J Radiat Res Appl Sci 7(4), 438-447.

[18] Myrick TE, Berven BA, Haywood FF (1983). Determination of concentrations of selected radionuclides in surface soil in the U.S. Health phys, 45, 631-642.

[19] Ali H. Taqi, Laith Abdul Aziz Al-Ani, Abbas M. Ali (2017). Estimating the natural and artificial radioactivity in soil samples from some oil sites in Kirkuk-Iraq using high resolution gamma ray's spectrometry. Indian journal of Pure and Applied physic, 55, 674-682.

[20] Hadi Al-Baidhani, Kadir GUNOGLU and Iskender AKKURT. (2019). Natural Radiation Measurement in Some Soil Sample from Basra oil field IRAQ State.

[21] Agbalagba, E.O., Avwiri, G.O. and Ononugbo, C.P (2013). Evaluation of naturally occurring radioactivity materials (NORM) of soil and sediments in oil and gas wells in western Niger delta region of Nigeria. Environ. Earth Sci. 70, 2613-2622.

[22] Ibraheim N. M., Shawky S., Amer HA (1995). Radioactivity levels in Lake Nasser sediments. Appl Radiat Isot 46(5), 297-299.

[23] Facchinelli A., Sacchi, E., & Mallen, L (2001). Multivariate statistical GIS-based approach to identify heavy metal sources in soils. Environmental Pollution, 114, 313-324.

[24] A. M. A. Adam, M. A. H. Eltayeb (2012), Multivariate statistical analysis of radioactive variables in two phosphate ores from Sudan. J Environ Radioactivity, 107, 23-43.

[25] Selin Özden (2021), Natural radioactivity measurements and evaluation of radiological hazards in sediment of Aliağa Bay, Izmir (Turkey).

[26] Suresh Gandhi M, Ravisankar R, Ravisankar R, Rajalakshmi A, Sivakumar S, Chandrasekaran A, Peram Anand D (2014). Measurements of natural gamma radiation in beach sediment of north east coast of Tamilnadu, India by gamma ray spectrometry with multivariate statistical approach. J Radiat Res Appl Sci, 7(1), 7-17.

[27] R Ravisankar, A. Chandrasekaran, Suganath Sivakumar, Prem Anand (2014). Measurement of Natural Radioactivity and Evaluation of Radiation Hazards in Coastal Sediments of East Coast of Tamilnadu using Statistical Approach.